AUV Propulsion and Maneuvering by Means of Asymmetric Thrust

Robin H. Littlefield[1], Frederic Jaffre[1], and Jeffrey W. Kaeli[1]

***Abstract*— We present an Asymmetric Propulsion System (APS) capable of generating both forward thrust and a lateral turning moment by means of a single-bladed propeller [1]. At constant rotational speeds, forward thrust is provided in the same manner as a symmetrical multi-bladed propeller. By varying the instantaneous rotational speed throughout each revolution, an off-axis thrust bias can be generated. We demonstrate how this can be used to control and maneuver an underwater robot and discuss its advantages and applications to autonomous underwater vehicle (AUV) design and operation.**

I. INTRODUCTION

The form factors and propulsion systems employed by unmanned underwater robots are largely driven by the tasks they perform. Figure 1 illustrates several classes of vehicles. Remotely operated vehicles (ROVs) receive power and control commands from an operator by means of a tether and are often tasked with performing fine scale manipulation. As such, they must be capable of holding station over an area of interest and often utilize an array of powerful thrusters capable of providing instantaneous thrust in any direction.

Autonomous underwater vehicles (AUVs), by contrast, are typically free-swimming, streamlined, and more often utilized for mapping a wide area or transiting long distances. The most streamlined AUVs generally rely on a single propeller to provide thrust and additional actuators to provide maneuverability. In order to remain at a desired depth, these vehicles must continuously move forward to counteract their buoyancy by maintaining flow over their bodies and control surfaces. In order to maneuver more slowly than this, additional thrusters can be added to provide directly control over vertical maneuverability. For example, slow speeds are desirable for building photomosaics that require large overlap between camera frames.

All of the aforementioned propulsion systems rely on propellers with multiple blades that are symmetrically distributed around the axis of rotation. The propeller rotates at a constant velocity, and the resulting thrust is proportional to the square of the propeller velocity. This thrust vector acts along the axis of the propeller shaft because of the symmetry in the blade distribution. In contrast, an asymmetric propulsion system (APS) can produce an average thrust vector that is off-axis of the propeller shaft and is thus able to provide both forward thrust as well as a turning moment for the vehicle [1]. The system is termed asymmetric because

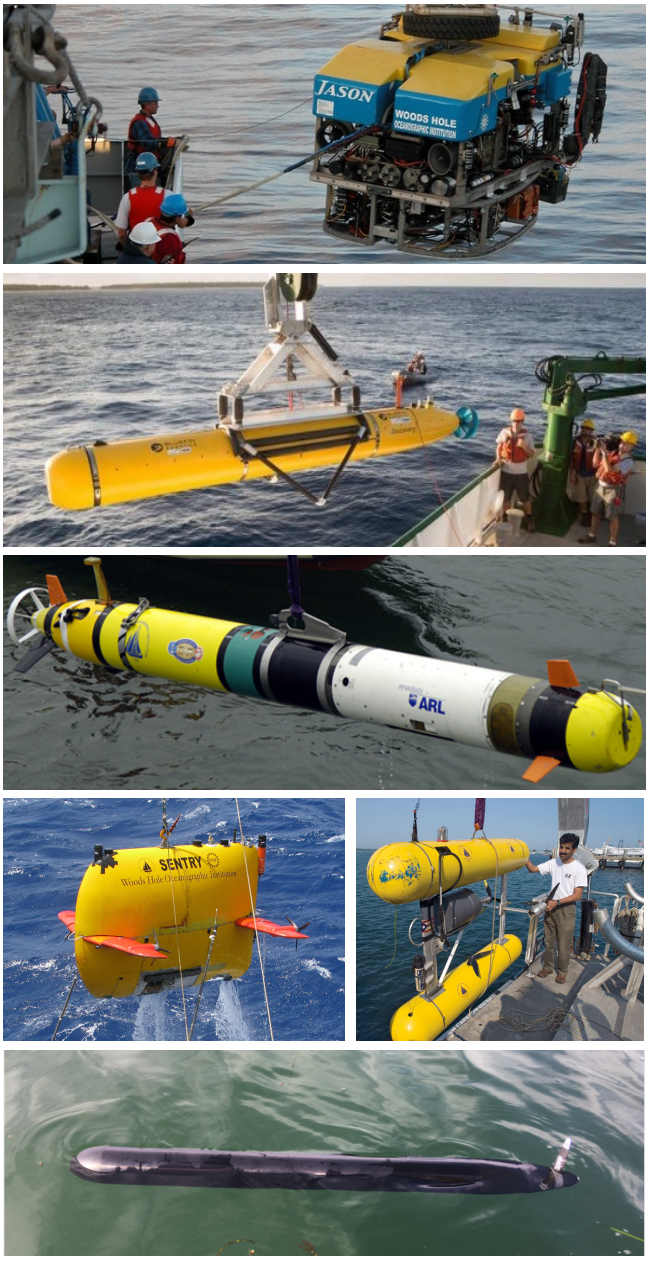

Fig. 1. A variety of unmanned underwater robots with a variety of propulsion systems for performing a variety of tasks. *From top to bottom:* ROVs like JASON are controlled by an operator over a tether and use a variety of thruster to hold station over areas of interest. AUVs are designed for long transits and large area searches are streamlined and can employ a vectored thruster like a Bluefin or a propeller with aft fins, and sometimes even forward fins, like a REMUS. AUVs designed as slow-moving and highly stable imagine platforms, like Sentry and SeaBed, use multiple thrusters to maintain low-speed maneuverability and have large separation between their centers of mass and buoyancy. The APS vehicle is designed to be both streamline and to maintain maneuverability at low speeds while only requiring a single degree of freedom asymmetric propeller to maneuver.

*This work has been funded thgouth WHOIs Access to the Sea Fund and the Office of Technology Transfer.

[1]The authors are with the Oceanographic Systems Laboratoty at the Woods Hole Oceanographic Institution, Woods Hole, MA 02543, USA {rlittlefield,fjaffre,jkaeli}@whoi.edu

the propeller blades are asymmetrically distrupted around the axis of rotation. In the case of the APS presented in this paper, the asymmetry arises from the use of a propeller with a single blade, but other manifestations with multiple asymmetrically distributed blades are possible as well.

This technology confers several advantages over traditional vehicle control systems. An APS is less complex, requiring fewer components, moving parts, and through-hull penetrations. This results in fewer failure modes and subsequently a lower overall system failure rate. It also enables a smaller overall physical footprint, making it an attractive choice for micro-AUV applications.

Furthermore, the use of actuated fins or other control surfaces creates additional drag. The elimination of these drag-generating features improves both speed and endurance of the vehicle which is critical in a system where available energy is limited [2]. In addition to contributing to a component of drag, pitch fins and rudders require flow over their control surfaces to be effective. An APS can maintain maneuverability without the requirement of forward motion to generate flow over control surfaces. The ability to travel and maneuver at low speeds dramatically reduces the power consumption of the propulsion system, increasing the mission duration and the linear coverage of the seafloor for a given power budget [3]. Asymmetric propulsion addresses all of these design concerns in an elegant and robust package, making it a compelling choice for building efficient and capable AUVs.

II. ASYMMETRIC PROPULSION

For any given fixed-pitch propeller, the thrust it generates is proportional to the square of its angular velocity. In an APS, the propeller blades are distributed asymmetrically around the axis of rotation. The thrust output can be increased or decreased in one sector by respectively increasing or decreasing the angular velocity throughout that sector during each revolution. As a result, the mean thrust vector over a revolution moves away from the central propeller axis. This thrust offset induces a turning moment that can be controlled to enable an AUV to go straight, turn to port or starboard, dive or climb, or any combination thereof.

Theory

Figure 2 shows the coordinate system and associated variables for an asymmetric propulsion system realized by a single bladed propeller. The x-axis is oriented forward, y-axis starboard, and z-axis down. The position of the single blade, shown in solid black, is measured by angle θ from the positive y-axis. The blade moves with instantaneous angular velocity ω. A simplifying assumption is made that the thrust force F of the propeller acts at a single point on the propeller blade, shown in grey, a distance r from the axis of rotation.

The nominal angular velocity $\bar{\omega}$ of the propeller is augmented asymmetrically throughout its rotation by a sinusoid of amplitude ω_A with a maximum velocity at θ_A.

$$\omega(\theta) = \bar{\omega} + \omega_A \cos\big(\theta - \theta_A\big) \tag{1}$$

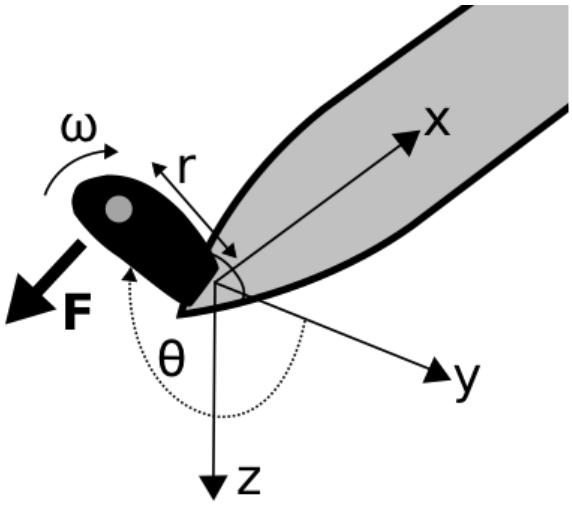

Fig. 2. Coordinate system diagram and associated variables for an asymmetric propulsion system realized by a single bladed propeller.

Constraints are placed on ω_A such that

$$0 \leq \omega_A < \bar{\omega}. \tag{2}$$

When $\omega_A = 0$ the propeller moves at a constant velocity and the system behaves identically to a traditional propeller providing forward thrust. In practice θ_A is controlled to determine the steering orientation, but it is now set to 0 for the sake of simplicity.

The instantaneous force $F(\theta)$ generated by the propeller blade is proportional to the square of the velocity ωr by some constant C. Integrating this force over one complete rotation provides a notional forward thrust $\bar{F}$ for the system.

$$\bar{F} = \int_0^{2\pi} C\big(r\omega(\theta)\big)^2 d\theta = \pi C r^2 \big(2\bar{\omega}^2 + {\omega_A}^2\big) \tag{3}$$

From this equation, it can be seen that increasing the asymmetric velocity amplitude ω_A increases the force even if the nominal velocity amplitude $\bar{\omega}$ remains constant. This additional force needs to be compensated by the motor controller when generating command signals.

The instantaneous pitch and yaw moments, $M_y(\theta)$ and $M_z(\theta)$, respectively, are equal to the instantaneous force multiplied by their respective instantaneous moment arms $z(\theta) = r\sin(\theta)$ and $y(\theta) = r\cos(\theta)$. Integrating this moment over one complete rotation provides a notional turning moment for the system.

$$\bar{M}_y = \int_0^{2\pi} C\big(r\omega(\theta)\big)^2 z(\theta) d\theta = 0 \tag{4}$$

$$\bar{M}_z = \int_0^{2\pi} C\big(r\omega(\theta)\big)^2 y(\theta) d\theta = 2\pi C r^3 \bar{\omega}\omega_A \tag{5}$$

For the current case of $\theta_A = 0$, the pitch moment is 0 since the upper and lower hemispheres are balanced, while the yaw moment is proportional to both velocity amplitudes.

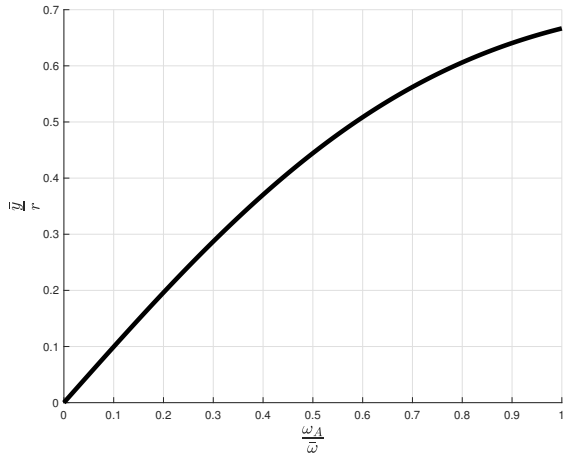

Fig. 3. Normalized moment arm as a function of velocity amplitude ratio. The diminishing return behavior of this relationship combined with the proportional relationship in Equation 5 suggests that operating at higher average RPM with smaller modulations of asymmetric amplitude will be more efficient than lower average RPMs and a higher asymmetric amplitude.

Normalizing the yaw moment by the force provides a notional moment arm $\bar{y}$ for the system.

$$\bar{y} = \frac{\bar{M}_z}{\bar{F}} = \frac{r\left(\frac{\omega_a}{\bar{\omega}}\right)}{1 + \frac{1}{2}\left(\frac{\omega_a}{\bar{\omega}}\right)^2} \tag{6}$$

This moment arm can in turn be normalized by the radius and plotted as a function of the amplitude ratio $\frac{\omega_a}{\bar{\omega}}$ as shown in Figure 3. The diminishing return behavior of this dimensionless relationship combined with the proportional relationship in Equation 5 suggests that operating at higher average RPM with smaller modulations of asymmetric amplitude will be more efficient than lower average RPM and a higher asymmetric amplitude.

A propeller rotating at a constant velocity will affect a constant torque on the vehicle body. This results in a static roll force that is typically compensated for via vertical separation of the center of gravity and center of buoyancy for passive stability, or by active roll control using additional control surfaces. A propeller rotating at a sinusoidally augmented velocity will additionally induce a sinusoidal torque on the vehicle body. If these occur at frequencies near the natural rolling frequency of the vehicle, the platform will be unstable. This is another case for operating at high RPM, well above the natural roll frequency of the vehicle.

Implementation

A thruster board was specifically developed to accurately control the speed of a motor through a full revolution with a 0.1° resolution at maximum of 3000 RPM. It is composed of a microcontroller and driver/power stage. Using two external sensors, a position sensor and a hall sensor paired with a magnet on the shaft for detecting the top position, the motor controller varies the angular speed of the propeller and tracks the response throughout the 360° revolution. The angular resolution is equal to the position sensors resolution. The host processor uses a serial port to communicate with the board to send commands and receive accurate and instant feedback of the position of the rotating propeller shaft. This allows the motor controller to vary speed while keeping track of the response.

The PIC32MK microcontroller unit (MCU) combines 32-Bit, 120 MHz performance with 1MB of Flash memory and a rich peripheral making it adequate for motor control applications. The microcontroller controls the speed of the motor by sending a Pulse Width Modulation (PWM) signal to a MOSFET driver. The response of the driver to a change in the PWM signal is 180ns of allowing it to handle large speed variation within a single rotation up to the maximum RPM. The motor and the output load are typically the limiting factors in the dynamic response of the propeller. The sensing of the shaft position and the instant velocity are achieved using the microcontroller embedded quadrature encoder module paired with an external magnetic encoder. This information allows the MCU to servo the speed by applying a correction to a PWM control table generated from the serial command. This table represents the velocity profile of one rotation. The index position is reset when the magnet, positioned in line with the single blade of the propeller, passes by the Hall-effect sensor. It takes approximately $5\mu s$ for the microcontroller to compute the instantaneous speed and the average RPM, then apply the necessary corrections to the PWM table. The quadrature encoder module features decimation and extrapolation capability providing the desired angle resolution.

The power stage is composed by a Texas Instrument DRV8306 device which is an integrated gate driver for 3-phase brushless DC motor applications. It provides three half-bridge gate drivers, each capable of driving the high-side and low-side of the N-channel power MOSFETs. The device generates the proper gate drive voltages using an integrated charge pump for the high-side MOSFETs and a linear regulator for the low-side MOSFETs. The DRV8306 has three Hall comparators which use the input from the Hall elements for internal commutation. The duty cycle ratio of the phase voltage of the motor is adjusted from a PWM signal generated by the PIC32 microcontroller. Two peripheral inputs pins are used for braking and setting the direction of the motor. A 3.3V, 30-mA low-dropout regulator supplies the motor position sensor and Hall elements. The driver provides an additional signal which is a measure of the commutation frequency. This signal is used for implementing the closed-loop control of the motor in applications that do not need variable rotational velocity. A low-power sleep mode is available to achieve low quiescent current draw by shutting down most of the internal circuitry. Internal protection functions are provided for under-voltage lock-out, charge pump fault, MOSFET over-current, MOSFET short-circuit, gate driver fault, and overtemperature. Fault conditions are indicated on an output pin allowing the microcontroller to take appropriate action in the event of a fault. The current limit is programmable and set by the microcontroller. It allows the board to limit the output torque

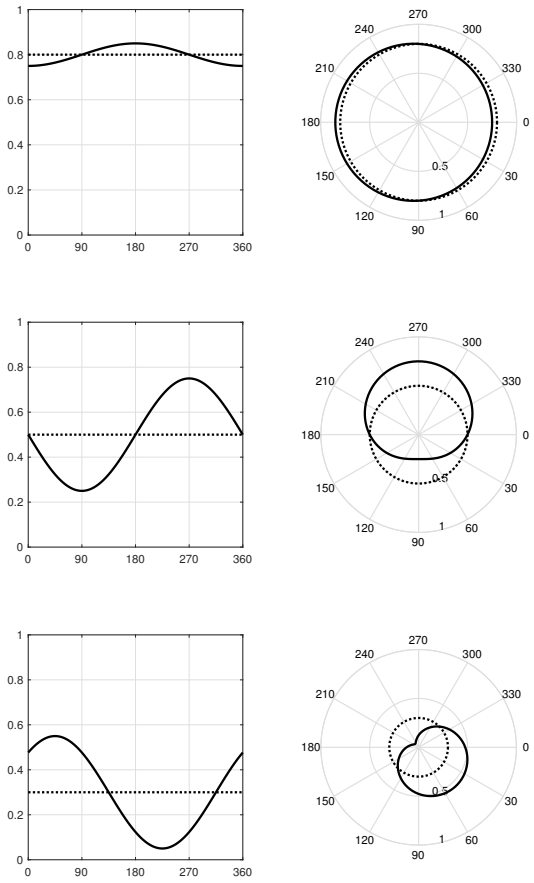

Fig. 4. Three sample control function in cartesian (*left*) and polar (*right*) space. The dotted line indicates the nominal component. *Top:* A slight turn to starboard at high speed. *Middle:* A pitch downward at moderate speed. *Bottom:* A simultaneous upward pitch and turn to port at slower speeds but equivalent asymmetric amplitude to the middle plot.

without shutting down the motor in overload situations. The CSD88584Q5DCT MOSFET used on the board are rated to 50A continuous when properly cooled. Passive cooling is achieved by adding a heat sink on the exposed pads.

To control the thruster, the host sends 4 parameters via the serial connection. The first two are proportional to the velocity amplitudes $\bar{\omega}$ and ω_A and are expressed as a percentage of the maximum power the motor controller can deliver. Due to the interdependency of the steering amplitude and the average RPM, the motor controller places restrictions on these values such that they must sum to 1, in addition to the constraint in Equation 2. The second parameter is the angle of maximum velocity θ_A, and the fourth is a Boolean value indicating clockwise or counter clockwise rotation. The motor controller rejects commands that do not follow these rules in order to prevent a clipping situation that would otherwise limit the maneuverability of the AUV as the maximum average RPM is approached. The motor controller board replies with the same message scheme representative of the actual response of the output shaft. Figure 4 shows several example control functions .

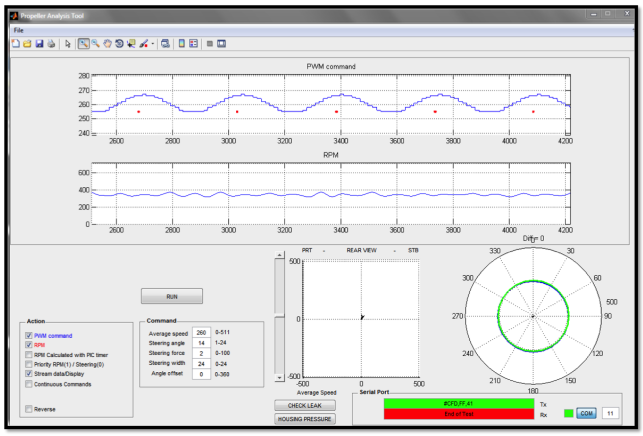

Fig. 5. A screen grab of the MATLAB control interface.

III. TESTING

Testing was performed at the Woods Hole Oceanographic Institution (WHOI) with the intention of proving the feasibility of maneuvering a streamlined body by means of an APS. Initial testing was conducted within a test flume, a long test tank allowing for ample viewing of vehicle behavior. Further testing was conducted in Great Harbor, the body of water adjacent to the WHOIs village campus.

Experimental Setup

To perform these demonstrations, a brushless DC motor was used to drive a single-bladed propeller. The motor was paired with an indicator magnet and a Hall Effect sensor to index the vertical position of the propeller upon each revolution. This system was housed in a streamlined cylindrical hull with fixed fins and was configured to perform two distinct tests both using a MATLAB control interface running on an external laptop computer. This interface was used to command the motor controller and send and display the propeller top position, the generated PWM command, the average speed, and the calculated average RPM. The first test consisted of a fixed tank test, shown in Figure 6, and the second test consisted of a free swimming test, shown in Figure 7. Tank testing was conducted by suspending the vehicle in a test flume by two vertical lines spaced on either side of the vehicle center of gravity. This test vehicle was ballasted to be negatively buoyant and thus take advantage of the support lines to maintain a fixed orientation and position in the center of the water column when uninfluenced by the thrust characteristics of the propulsion system. Open water testing was conducted by rigidly attaching the test vehicle to a buoyant foam surface float such that the vehicle would remain submerged at a constant depth but was free to maneuver laterally.

Methods

The experiments performed in the test flume were conducted with the thruster running at low average RMP such as to limit the forward motion of the suspended vehicle. The computer running MATLAB control code was connected to

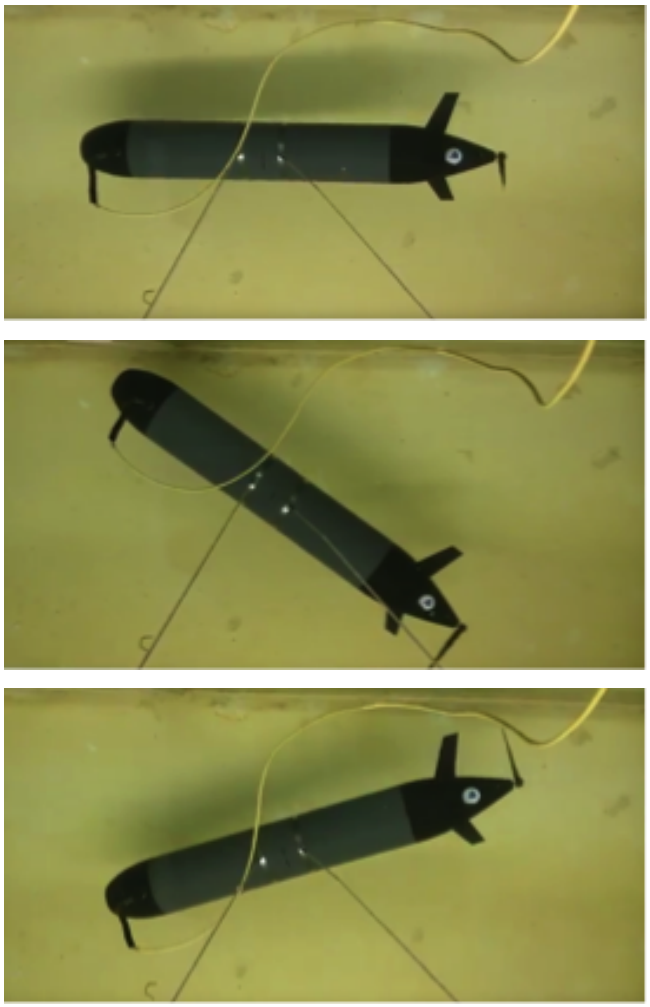

Fig. 6. Tank testing with the vehicle at rest (*top*), turning to starboard (*middle*), and turning to port (*bottom*) while controlled via a tether.

the vehicle motor controller in the test housing by means of an underwater cable and used to send commands to control asymmetric thrust output. Open water tests were run at higher average RPM to generate a realistic representation of typical survey speeds. An additional electronics housing with Wi-Fi communfication was attached to the surface float which was connected to the vehicle via an underwater cable. In this manner commands could be sent over Wi-Fi to the vehicle from a laptop computer to allow untethered control of vehicle movement while maintaining a fixed depth and surface expression for tracking and communication.

Conclusions

We convincingly demonstrated that a thrust bias can be introduced such as to induce and maintain a turning moment and influence the yaw of the vehicle. In tank tests the vehicle could be commanded to make and maintain turns to port and starboard. In open water testing vehicle speeds between 1.5 and 1.8 m/s were demonstrated and turning radii less than 15m could be achieved at these speeds. Multiple figure eight patterns were repeated and the test vehicle was controlled remotely to transit from a floating dock to the operating area

Fig. 7. Open water testing in the harbor adjacent to the WHOI pier.

and back again for recovery. These demonstrations show that this technology can be practically applied to achieve speed and control comparable to that of existing AUVs.

IV. DISCUSSION

We have successfully proven the concept of asymmetric propulsion and demonstrated its ability to be harnessed to control the movement of an underwater robot. APS technology addresses several key issues in the space of AUV design including size, complexity, drag and maneuverability, all of which contribute significantly to endurance and capability. It allows vehicles to maintain maneuverability throughout a full range of speeds, and a vehicle utilizing an APS may be capable of orientating itself at very low speeds without the need for additional thrusters. This type of low-speed maneuverability could enable an AUV to hold station, hover, and enter low-power loiter behaviors. They also have the potential to offer improvements in efficiency, reliability, and cost as compared to existing propulsion and maneuvering systems.

An APS could potentially be realized on an AUV tasked with finding the wreckage of a downed airplane and searching for the flight recorder. An APS would enable the AUV to make a low-speed, energy efficient transit to the suspected site, then speed up to the optimal speed for a sonar survey. Upon detecting potential targets, the AUV could drop in altitude, maneuvering slowly over each one while capturing high-resolution imagery and stitching together three-dimensional models of the objects. If one of these objects is determined to be the flight recorder, the AUV could then hover over the recorder, cutting it free of debris and picking it up with a manipulator arm before returning the recorder to the surface. This single-mission paradigm would dramatically reduce the costs of operations that currently require multiple missions with multiple different classes of robotic vehicles, and it could potentially eliminate the need for a surface support ship as well.

Asymmetric propulsion is a key enabling technology that will propel the next generation of marine robots. These platforms will have enhanced autonomous capabilities, extended endurances, and be endowed with novel ways to interact with their environments. At the same time they must be matched with equally capable hardware and propulsion systems that will maximize the utility of these new developments. We see great utility for asymmetric propulsion, not only as an enabler in high-end AUVs, but also as a simplifying cost-saving factor in smaller, low-cost systems that will ultimately make AUVs more egalitarian and bring their utility to a broader user base.

ACKNOWLEDGMENT

We would like to recognize Tom Austin, Ben Allen, and Mike Purcell for their helpful insight throughout this work

REFERENCES

[1] T. Austin, M. Purcell, F. Jaffre, J. Kaeli, B. Allen, and R. Littlefield, "Asymmetric propulsion and maneuvering system," U.S. Patent 873499B2, January 2018.

[2] B. Allen, W. S. Vorus, and T. Prestero, "Propulsion system performance enhancements on remus auvs," in *Oceans 2000 MTS/IEEE Conference and Exhibition*, vol. 3. IEEE, 2000, pp. 1869–1873.

[3] H. Singh, D. Yoerger, and A. Bradley, "Issues in auv design and deployment for oceanographic research," in *Robotics and Automation, 1997. Proceedings., 1997 IEEE International Conference on*, vol. 3. IEEE, 1997, pp. 1857–1862.